Effects of Local Eccentricity of Connecting Braces on Nonlinear Behavior of Steel Concentric Brace Connections

B. Hosseini Hashemi[1], F. Behnamfar[2], and F. Ranjbaran[3]

1. Assistant Professor, Structural Engineering Research Center, International Institute of Earthquake Engineering and Seismology, I.R. Iran, email: behrokh@iiees.ac.ir
2. Assistant Professor, Isfahan University of Technology, Isfahan, I.R. Iran
3. Ph.D. Student, Islamic Azad University, Tehran, I.R. Iran

ABSTRACT: *According to most current building codes, in order to prevent a steel brace from brittle behavior due to buckling, it is necessary to use prescribed stronger and stiffer sections. However, experience from past earthquakes has shown that the above requirement is not effective in containing the brittle failure of members, not even in postponing this unwanted behavior. It is well known that one of the factors affecting dynamic behavior of a brace is its end condition, i.e., the stiffness of connection plates known as gusset plates (GP). In this paper through numerical simulation it is suggested to offset the connecting members at the connection to enhance the ductility and even strength of the connection itself. For the purpose of this research work, numerical models are studied using nonlinear static analysis. A very good match is shown to exist between results of computer simulation and experimental results, making it possible to study much more models at less time, effort, and cost, comparing to experimental work. A summary of results from numerical modeling and nonlinear analysis on 5 different connection configurations of cross and chevron bracing is also given and compared. It was shown that the eccentricity at connecting point is resulted in increasing ductility.*

Keywords: Brace connections; Nonlinear behavior; Local eccentricity; Steel

1. Introduction

Connections are of prime importance in steel structures that usually are neglected in analysis and design of structures whereas can be resulted in collapse of buildings having inconsistent design of their steel connections. This research work is focused on connections of cross and chevron bracing in concentric braced frames (*CBF's*).

Past research and experiments has revealed that three parameters shape the hysteretic behavior of bracing members, namely, member slenderness ratio, its end connections, and, geometry of its cross section [1-2]. According to most of these research works, out-of-plane buckling of connection plates [2-3] and also inappropriate formation of the plastic region on these plates [4-5] result in reduction of load capacity and ductility of brace members. Because of this, recommendations have been given to increase the overall ductility through limiting in-plane as well as out-of-plane buckling of gusset plates. To curb the out-of-plane buckling, ratio of the thickness of the connection plate to the free length of its edge has been specified [3]. Concerning the out-of-plane buckling of bracing members, a distance of at least two times the thickness of connection plate between the end of the brace and plate diameter has been suggested to augment the hysteretic energy dissipation. Keeping this distance long enough results in unrestrained formation of the plastic region in the gusset plates [5].

Therefore it is seen that gusset plates play a very important role in how the brace members behave especially under seismic loads. Accordingly, in this study theoretical models of the connections are tried to enhance the ductility of the connection system through avoiding the out-of-plane buckling of the gusset plates and letting the free formation of plastic region on the connection plates under seismic loads. A parameter of most importance here is the offset (eccentricity) of the brace member from the beam-column joint. Building codes do not suggest making a deliberate eccentricity in these connections but various experimental results have shown that existence of such an eccentricity in the above joints not only does not weaken the structural system they are part of which, but also modifies and enhances its dynamic behavior.

At first the experimental set-up by Gross [6] on cross bracing is studied. Eccentricity in Gross's model was created by transferring the longitudinal axis of the brace member from the intersection of beam and column axes to the top corner of the connecting plate where beam and column flanges meet, see Figures (3) and (4). This way the *GP* becomes more restricted regarding its free portions postponing the buckling in the plate. Then, the experimental models of Astaneh-Asl [7] are examined. Eccentricity in these models is generated first by intersecting the axes of chevron braces on the weld line connecting *GP* to top flange of the beam, and then by shifting this intersection point above the weld line, see Figures (7) and (8). This procedure replaces the brittle behavior of *GP* in local buckling to a nonlinear shear behavior which is ductile in essence.

With attaining numerical models that could be approved by experimental models one can save time and cost with less effort in modeling and to achieve sensitivity analysis on studying parameters.

In this paper after reviewing the results of past experiments, the above experimental models are analyzed using the static nonlinear analysis method (push-over). The purpose is to study the extent of enhancement of connection behavior due to deliberately generating an eccentricity in the connecting members in form of numerical model.

2. An Overview of the Past Experimental Modeling

In this section some of the past experimental works are reviewed.

In the case of cross bracing, the braced frame selected to be studied was a frame with diagonal bracing, shown in Figure (1a) [6]. A portion of this frame was adopted for experimental purposes and is shown in Figure (1b) with its boundary conditions and loading. In this experiment the loading was applied to the model monotonically.

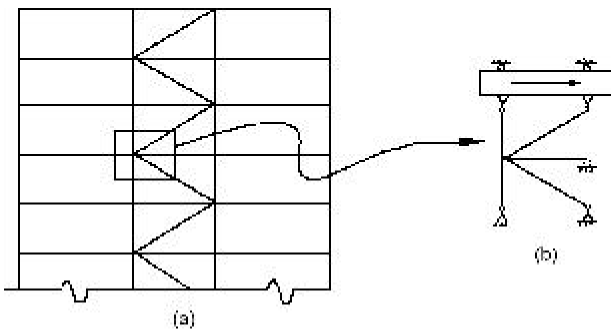

Figure 1. The experimental models. (a) The frame with diagonal bracing, (b) the experimental setup [6].

The dimensions of the experimental model are shown in Figure (2). In Figures (3) and (4), the section properties of the members with and without eccentricity are shown, respectively. The *GP's* and connection angles are of *A*36 and other members are of *A*441 steel. The connection of *GP* to the brace and column is bolted using high-strength *A*325 bolts and to the beams is welded using *E*70 electrodes.

The results of the experiments on the above diagonal bracing system are in the form of lateral force versus lateral displacement of the model (refer to Figure (1b)) and are shown in Figures (5) and (6)

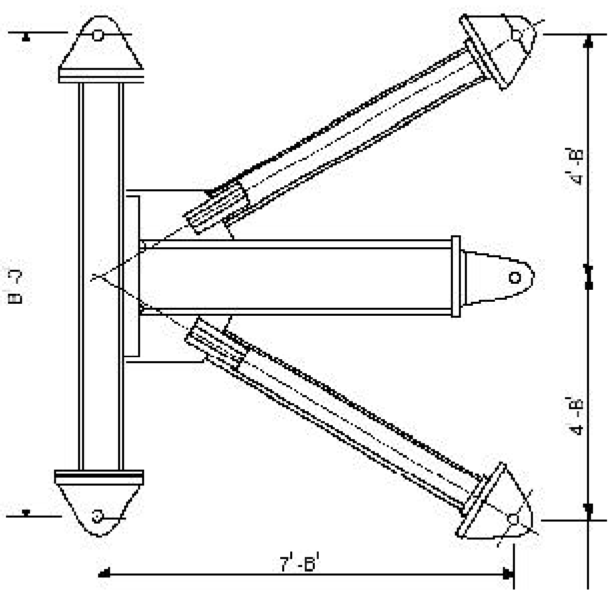

Figure 2. The dimensions of the experimental model of diagonal bracing [6].

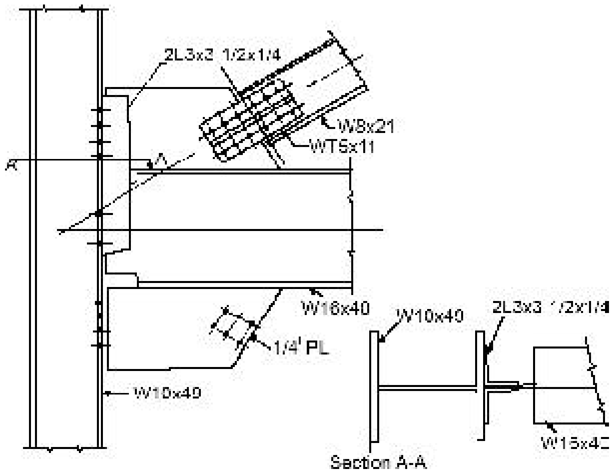

Figure 3. The section properties of the concentric model of diagonal bracing [6].

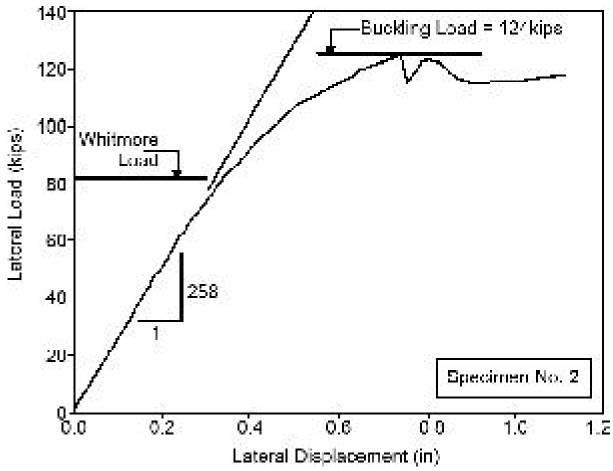

Figure 6. Experimental force-displacement curve for the eccentric diagonal bracing set-up [6].

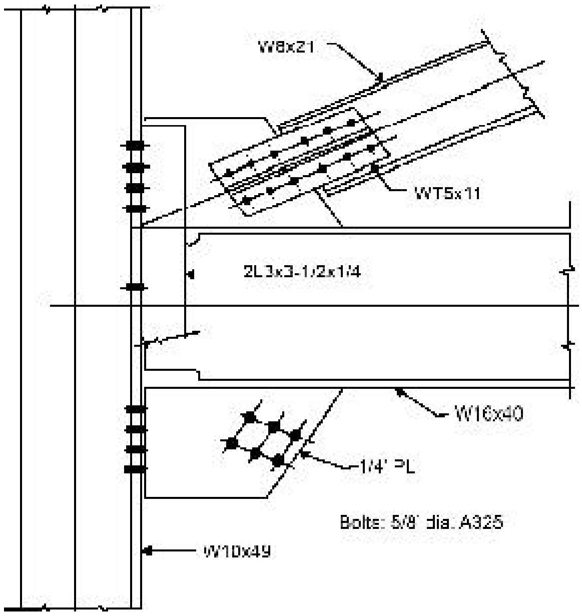

Figure 4. The section properties on eccentric model of diagonal bracing [6].

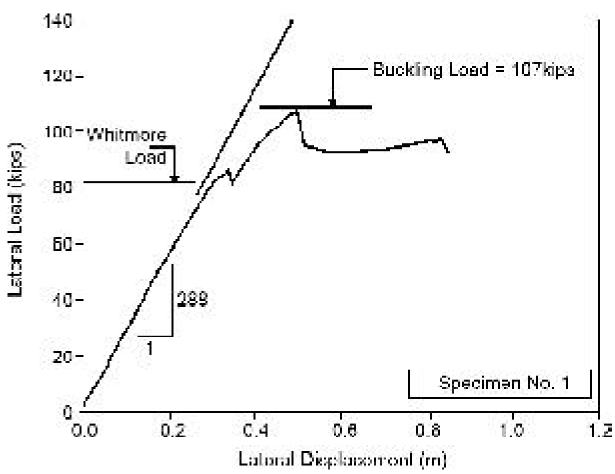

Figure 5. Experimental force-displacement curve for the concentric diagonal bracing set-up [6].

corresponding to models shown in Figures (3) and (4), respectively.

For the chevron bracing, the geometrical proportions are shown for concentric bracing in Figure (7) and for eccentric bracing intersecting on the weld line of *GP* to the beam and intersecting 2" above this line in Figures (8a) and (8b), respectively [7]. The *GP's* are of *A*36 and others are of *A*441 material. The model was subjected to a cyclic lateral displacement.

The experimental results of the chevron bracing as hysteretic loops of shear versus lateral deformation of connection *GP* is shown in Figure (9) for the concentric model, and for the eccentric models with braces intersecting on the weld line of *GP* to beam and 2" above this line.

3. Numerical Modeling

Ansys (5.4) program was used in this research. This program is able to take into account both the material and geometrical nonlinear characteristics of materials and members in analysis. The system is modeled using nonlinear shell elements having elastoplastic behavior. This element is suitable for analysis of small to medium thickness plates. Being a 4-node element with 6 degrees of freedom per node (translation in the direction of and rotation about *x*, *y*, and *z* axes), this element is adequate for nonlinear analysis subject to large rotations and strains. The analysis is nonlinear static under increasing loads in which large deformations and out-of-plane displacements are considered. Assuming that the strengths of connecting members are smaller than the connection itself and those of the connection plates are smaller than the connection welding, the connecting members fail

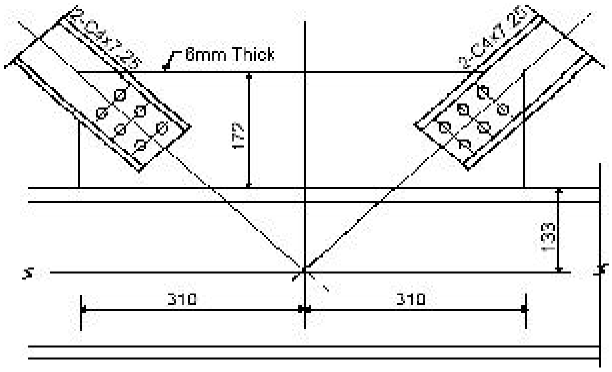

Figure 7. The geometrical proportions of the concentric chevron bracing [7].

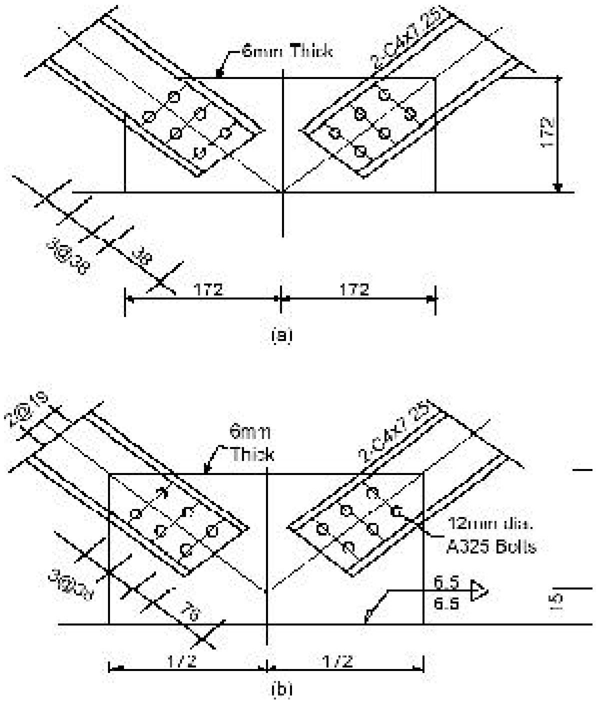

Figure 8. Dimensions of the eccentric chevron bracing. (a) Braces intersecting on the weld line of GP to the beam, (b) braces intersecting above the GP to beam weld line [7].

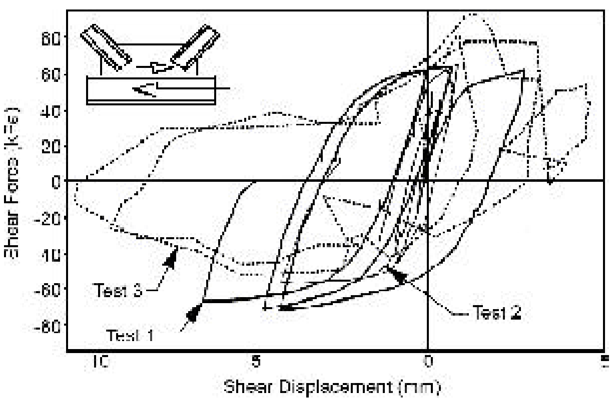

Figure 9. The hysteretic loops of shear versus lateral deformation of connection GP for the concentric chevron bracing (TEST3), eccentric chevron bracing on the weld line of GP to beam (TEST2), and braces intersecting 2" above the GP to beam weld line (TEST1) [7].

first. Therefore the welds of the connection are not modeled explicitly and displacement restrictions are enforced on the plate nodes along weld lines. The modulus of elasticity is 200*GPa* (29,000*ksi*) and the Poisson ratio is 0.3. The Von Mises yielding criterion and isotropic behavior for materials is assumed. The diagram of stress-strain of steel materials used is considered to be trilinear [3].

The finite-element meshes of concentric and eccentric models are shown in Figures (10a) and (10b), respectively. The boundary conditions in the cross bracing model is that the end points of the above column and brace are constrained to each other and are free in the horizontal direction. The beam is roll-ended while the lower column and brace are pin-ended, see Figures (10a) and (10b).

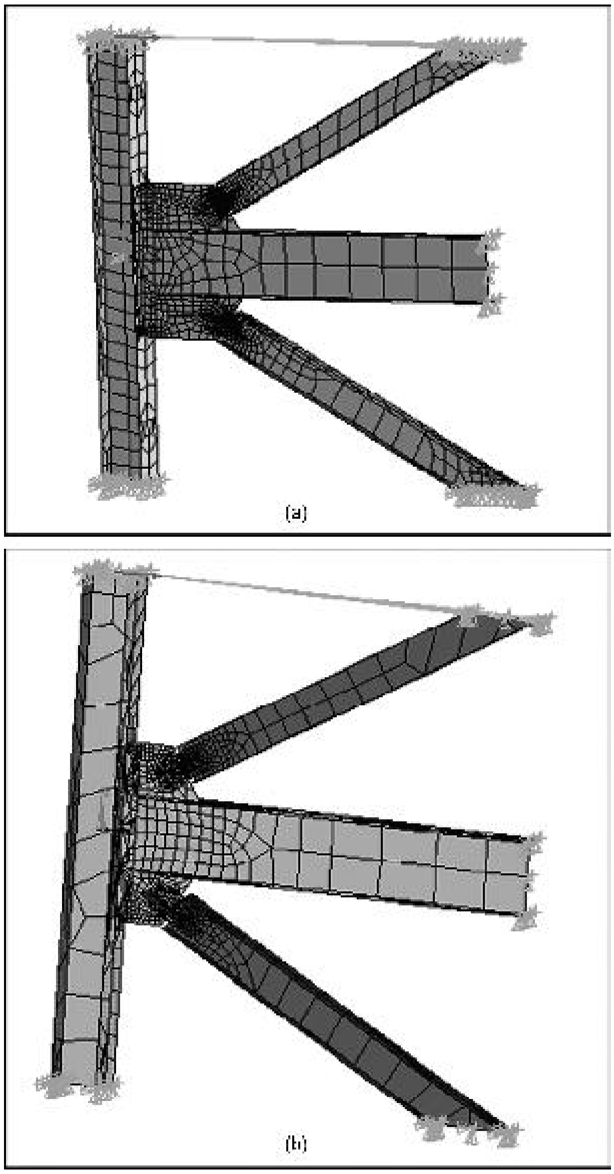

Figure 10. The finite-element mesh of the cross-bracing model. (a) Without eccentricity, (b) with eccentricity.

The boundary conditions in the model of chevron bracing are so that brace supports are hinged and those of beams are rolled. Also to be able to concentrate on the gusset plate's behavior, the nodes on the opposite ends of the beam are constrained together in the x-direction, see Figures (11) and (12).

4. Numerical Results

An increasing horizontal force is applied along the line intersecting the end points of the upper column and brace, see Figure (10), and the nonlinear force-displacement (push-over) curves are computed. Based on the experimental results described in the above section, the upper bound of the horizontal force is taken to be 533*kN* (120*kips*) for the cross bracing system. The model without eccentricity encountered a strength degradation resulting in divergence of the calculations. Because of this problem, the limit of the horizontal force in analysis of this model was decreased to 489*kN* (110*kips*), again without success. Finally a displacement-controlled analysis was successfully accomplished choosing a limit of 10*mm* (0.4*inch*) which was the ultimate displacement of the model with eccentricity. The results are shown in Figure (13).

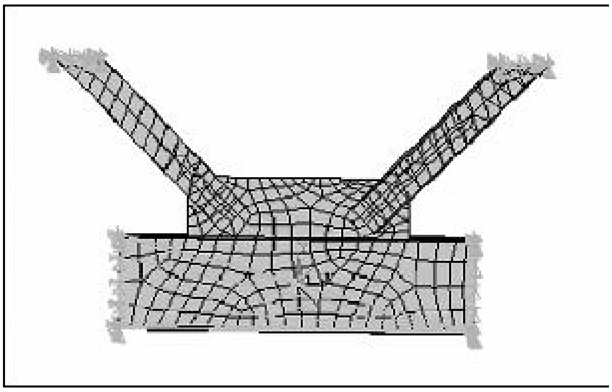

Figure 11. The finite-element mesh of the concentric chevron bracing model.

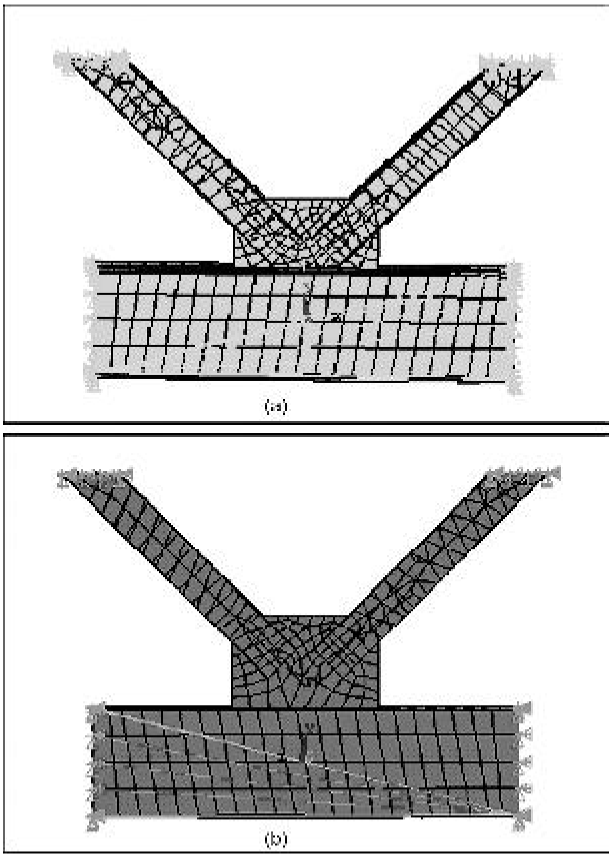

Figure 12. The finite-element mesh of the eccentric chevron bracing. (a) Braces intersecting on the weld line of GP to the beam, (b) braces intersecting above the GP to beam weld line.

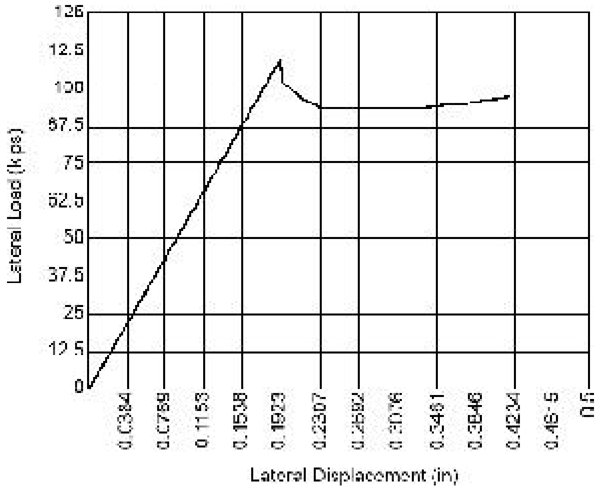

Figure 13. The calculated lateral force-displacement curve of the cross-bracing model without eccentricity.

Considering Figure (13), it is observed that for cross-bracing model with no eccentricity, the model exhibits a linear behavior up to a lateral force equal to 480*kN* (108*kips*). At this point, it shows a strength degradation and the applicable lateral force decreases to 417 *kN* (93.75*kips*). It should be noticed here that no strain hardening is seen and the maximum out-of-plane displacement of *GP* at the ultimate failure is 4.71*mm* (0.18527*inch*), see Figure (14).

Using the 533*kN* (120*kips*) limit value for the lateral force, the model with eccentricity, see Figure (10b) was analyzed without any problems and the resulting curve is shown in Figure (15).

Observing Figure (15) for cross-bracing with eccentricity, the model shows a linear behavior until the lateral force reaches 389*kN* (87.5*kips*). After exhibiting a nonlinear behavior up to 500*kN* (112.5*kips*), a local failure occurs and the lateral force decreases

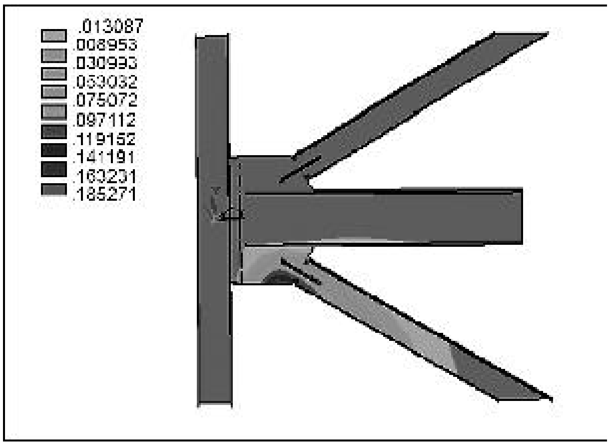

Figure 14. Distribution of out-of-plane displacement of GP for the concentric cross-bracing under monotonic loading at failure.

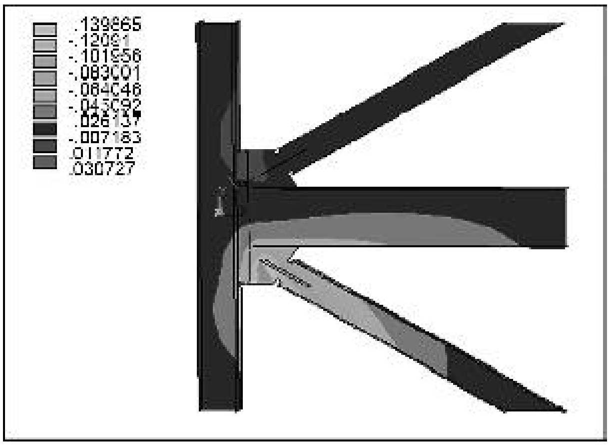

Figure 16. Distribution of out-of-plane displacement of GP for the eccentric cross-bracing under monotonic loading at failure.

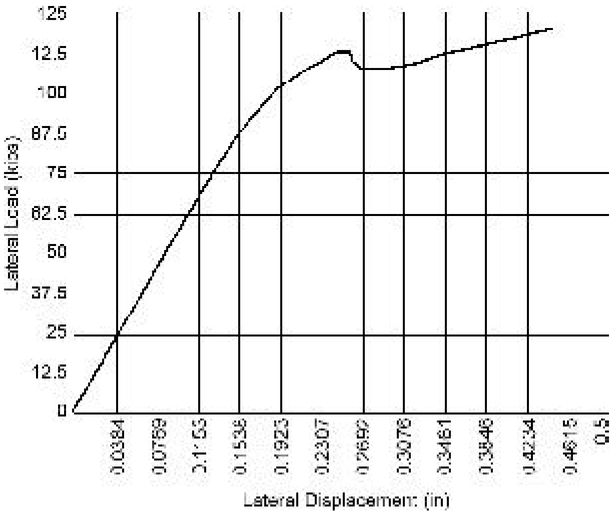

Figure 15. The calculated lateral force-displacement curve of the cross-bracing model with eccentricity.

to 475*kN* (107*kips*). Strain hardening results in an increase of lateral force to 533*kN* (120*kips*) afterwards. The maximum out-of-plane displacement in *GP* at ultimate failure is 3.55*mm* (0.13986*inch*), see Figure (16).

Comparing Figures (13) and (15), it can be observed that the behavior of concentric cross-bracing system is linear until a sudden buckling type occurs. Then a residual strength remains in the model up to ultimate displacement. On the other hand the behavior of eccentric cross-bracing is similar to snap-through buckling in shells with less stiffness and yielding before buckling in comparison with the last model and a positive stiffness with a stable behavior is seen in force-displacement diagram of the system after a local buckling at *GP* edges. This behavior results in an increased strength and ductility in cross-bracing system with eccentricity that can be resulted from decrease of free edge length and resulted in increase of buckling strength of gusset plate.

The chevron bracing models, at first are assessed using a monotonic push-over analysis. To avoid stress concentration, the lateral load is uniformly applied along the height of the beam equal to 447.5*kN* (100.7*kips*). Considering the results of the experiments, the maximum lateral displacement in the model without eccentricity was selected as 25.4*mm* (1*inch*); in the model with eccentricity with braces intersecting on the weld line of *GP* to beam as 63.5 mm (2.5*inch*); and with eccentricity of 2" above this line as 127*mm* (5*inch*), respectively. The results are shown in Figures (17) and (18).

Regarding Figure (17) for the concentric chevron bracing, it is observed that the model encounters a total failure at a lateral displacement of 17.8*mm* (0.7*inch*) with the lateral load equal to 205.8*kN* (46.3*kips*) that can be resulted from out-of-plane displacement of gusset plate. The force-displacement diagram continues with a negative slope after this displacement point. The out-of-plane movement of the *GP* of compressive brace at the last step of loading in push-over analysis is 40.61*mm* (1.599*inch*), see Figure (19).

In spite of largeness of *GP* dimensions, distribution of plastic strains is concentrated in a small zone at horizontal and vertical edges of plate next to the bracing member. This phenomenon shows that the total capacity of the plate for energy dissipation is not mobilized, see Figure (20) and that the governing behavior is a brittle one of lateral buckling type.

It is seen in Figure (18a) that in the chevron bracing with eccentricity on weld line, lateral displacement of the system in excess of 63.5*mm*

(2.5*inch*) without degradation of strength makes some difficulties in analysis which results in divergency of the analysis. This can be resulted from some strength degradation in the system. However, due to nonlinear

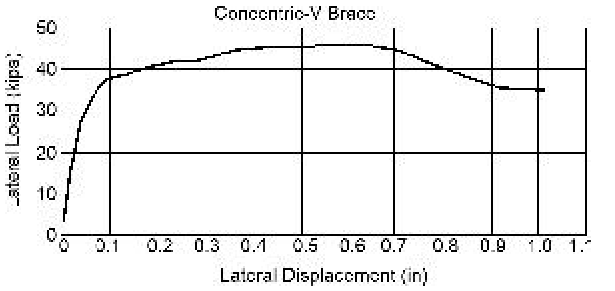

Figure 17. The calculated lateral force-displacement curve of the concentric chevron bracing model.

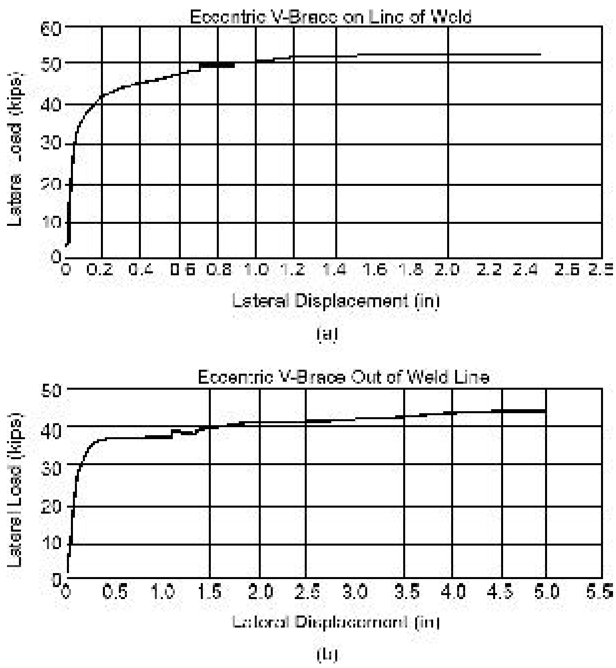

Figure 18. The calculated lateral force-displacement curve of the eccentric chevron bracing model. (a) Braces intersecting on the weld line of GP to the beam, (b) braces intersecting above the GP to beam weld line.

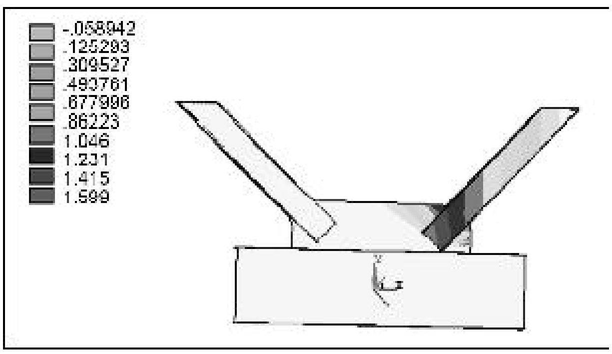

Figure 19. Distribution of out-of-plane displacement of GP for the concentric chevron bracing under monotonic loading at failure.

shear deformations no sudden failure occurs and only the slope decreases to about zero. The limiting load value is 238*kN* (53.5*kips*). The out-of-plane displacement of *GP* at the last step of loading of push-over analysis at the compressive brace is 2.34*mm* (0.092*inch*), see Figure (21), which shows an important decrease in out-of-plane displacement, elimination of buckling, and dominance of nonlinear shear behavior in the *GP*.

Distribution of plastic strains shows that most of the region between brace's end and beam flange has yielded and behaved nonlinearly, see Figure (22), which again is a reason for dominance of nonlinear shear behavior.

Regarding Figure (18b) for chevron bracing model with an eccentricity of 50.8*mm* (2*inch*) above *GP* weld line in push-over analysis, it was seen that the model can easily accommodate a lateral displacement of 127*mm* (5*inch*). The slope of force-displacement curve becomes zero at this point and the corresponding lateral load is 198*kN* (44.5*kips*). It is noteworthy to see that the value of

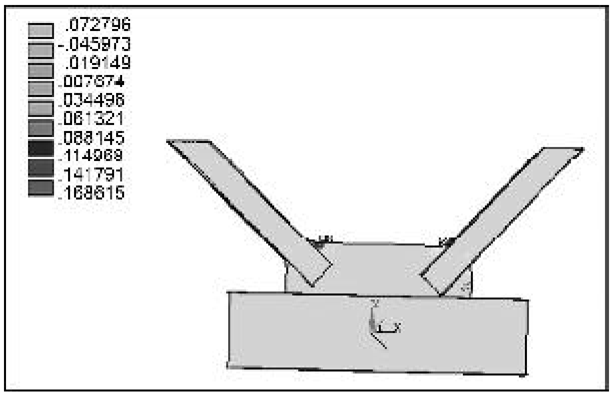

Figure 20. Distribution of plastic strains in the GP of concentric chevron bracing.

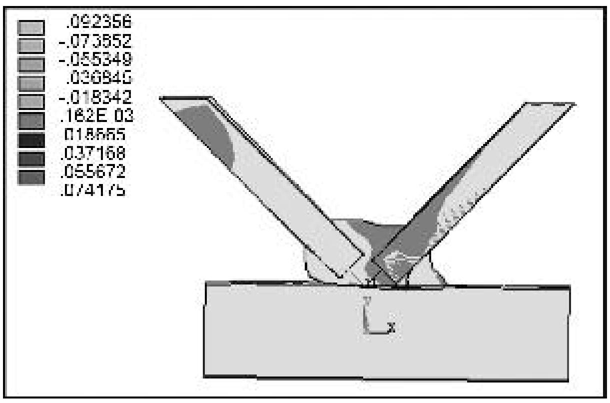

Figure 21. Distribution of out-of-plane displacement of GP for the chevron bracing eccentric on GP weld line under monotonic loading at failure.

out-plane displacement of *GP* at the last step of load in push-over analysis is limited to a maximum of 2.54*mm* (0.1*inch*), see Figure (23).

Distribution of plastic strains shows that the *GP* is in completely yielded state in a zone between the ends of braces and the beam flange and has entered the plastic region, see Figure (24).

The phenomenon seen in the above figure demonstrates a nonlinear shear behavior in the *GP* and shows a lateral displacement equal to two times that of the model eccentric on the *GP* weld line. The comparison between concentric and eccentric above weld line in chevron bracing shows that the eccentricity results in more ductility and dissipation of energy. This is because of the decrease of free edge length of gusset plate and the existence of region between intersection of brace axes and weld line. With decreasing free edge length the strength of buckling increases, in the other hand the mentioned region acts in the form of a ductile fuse similar to eccentric bracing. Therefore the capacity design method can govern in the analysis and design.

Observing the cyclic behavior and to evaluate the level of energy dissipation, the models were subjected to lateral displacement reversals of beam. This displacement was $\pm$ 5.08*mm* ($\pm$ 0.2*inch*), $\pm$ 10.16*mm* ($\pm$ 0.4*inch*), and $\pm$ 15.24*mm* ($\pm$ 0.6*inch*) in the first, second, and third cycles, respectively. The results are demonstrated in Figures (25) and (26). The comparison between Figures (25) and (26) show that hysteretic loops become more stocky and regular with increasing eccentricity at connecting members. This process shows the dissipation of energy increases with arising eccentricity. This subject is approved by monotonic analysis too. This behavior results from shear yielding and decrease of out of plane displacement of gusset plate.

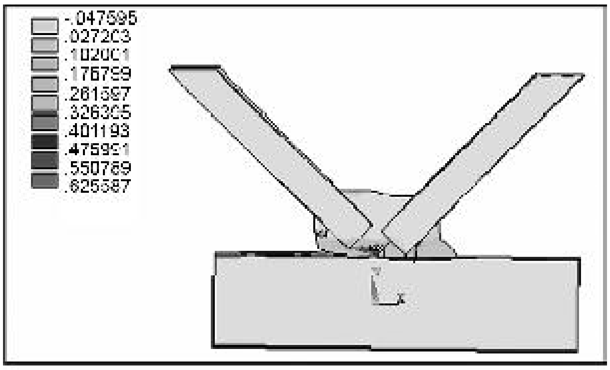

Figure 22. Distribution of plastic strains in the GP of chevron bracing eccentric on the weld line.

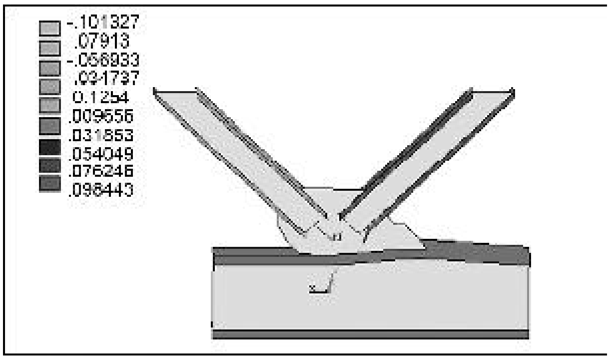

Figure 23. Distribution of out-of-plane displacement of GP for the chevron bracing eccentric 2in. above the GP weld line under monotonic loading at failure.

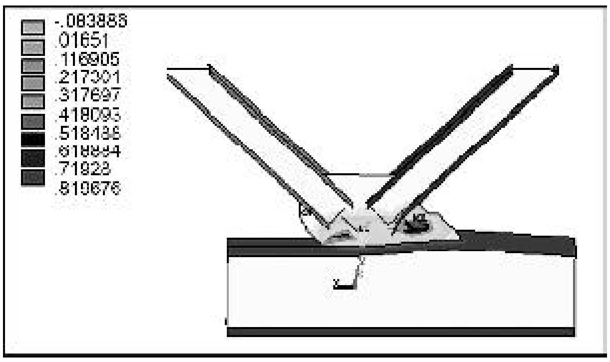

Figure 24. Distribution of plastic strains in the GP of chevron bracing eccentric 2in. above the weld line of GP.

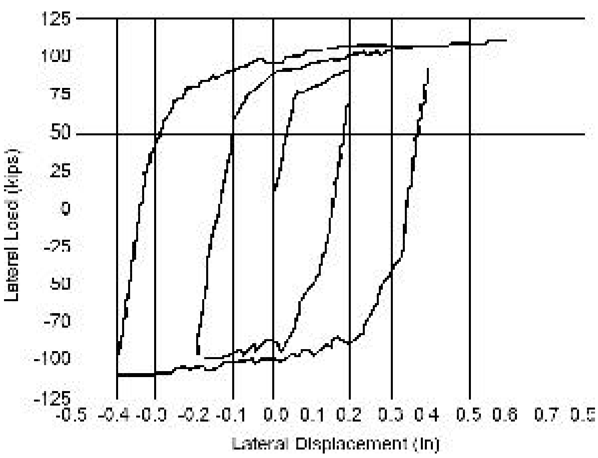

Figure 25. The hysteretic loops of lateral force versus lateral deformation of the concentric chevron bracing model.

5. Conclusions

The effects of eccentricity of connecting members of a steel brace-beam-column connection and the behavior of its connection plate (gusset plate, or, *GP*) were studied.

The numerical results derived from nonlinear finite element modeling and analyses in this study are in

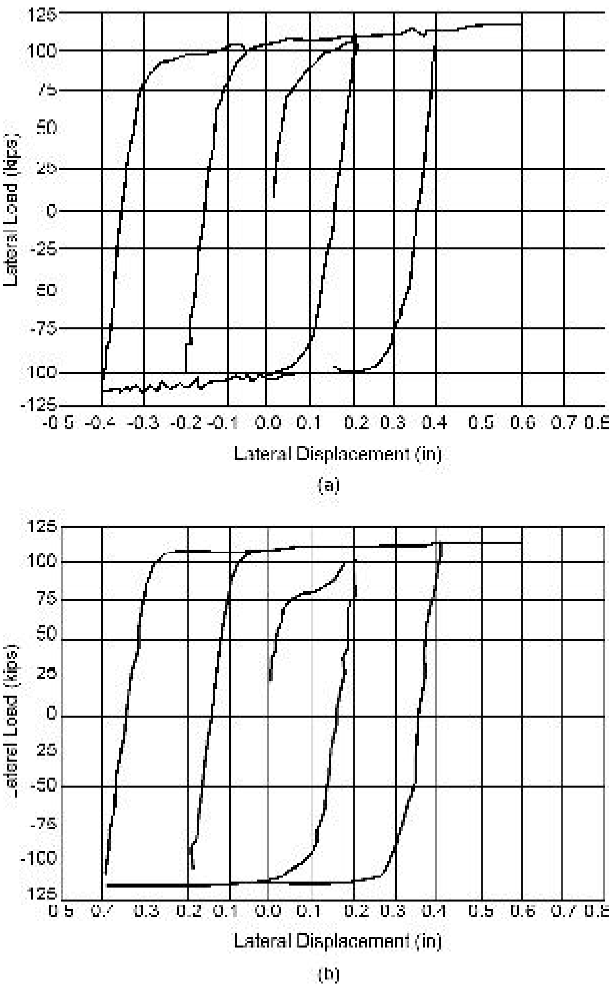

Figure 26. The hysteretic loops for the eccentric chevron bracing. (a) Braces intersecting on the weld line of GP to beam, (b) braces intersecting 2" above the GP to beam weld line.

good agreement with the experimental results.

Eccentricity at connecting cross-bracing was resulted in increasing of ductility. As it is apparent, the ductility and strength are more superior such that buckling displacement of the *GP* in the out-of-plane direction decreases 32% and load resistance increases 11% and the lateral stiffness decreases too.

In chevron models, considering their lateral force-displacement behavior, and hysteretic loops, it is observed that with increasing eccentricity related to weld line the ductility is increased too. This increase of ductility is caused by limited out-of-plane deformation, extension of plastic strains on a larger surface of *GP*.

References

1. Bruneau, M., Uang, Ch-M., and Whittaker, A. (1998). "Ductile Design of Steel Structures", First Ed., McGraw-Hill.

2. Bjorhovde, R. and Chakrabarti, S.K. (1985). "Tests of Full-Size Gusset Plate Connections", *Journal of Structural Engineering, ASCE*, **111**(3), 667-684.

3. Yamamoto, K., Akiyama, N., and Okumura, T. (1988). "Buckling Strength of Gusseted Truss Joints", *Journal of Structural Engineering*, **114**(3), 575-590.

4. Astaneh-Asl, A. and Goel, S.C. (1990). "Cyclic In-Plane Buckling of Double Angle Bracing", *Journal of Structural Engineering, ASCE*, **110**(9), 2036-2055.

5. Astaneh-Asl, A., Goel, S.C., and Hanson, R.D. (1985). "Cyclic Out-of-Plane Buckling of Double Angle Bracing", *Journal of Structural Engineering, ASCE*, **111**(5), 1135-1153.

6. Gross, J.L. (1990). "Experimental Study of Gusseted Connections", *AISC Structural Engineering Journal, 3rd Qtr.*, **7**, 1990, 89-97.

7. Astaneh-Asl, A. (1999). "Cyclic Tests and Seismic Design of Steel Gusset Plates in Buildings", *Proceedings of the 3rd International Conference on Seismology and Earthquake Engineering (SEE3)*, Tehran, I.R. Iran.